

**Circular photogalvanic effect induced by near-infrared radiation in InAs quantum wires patterned quasi two-dimensional electron system**Chongyun Jiang,<sup>1</sup> Yonghai Chen,<sup>1, a)</sup> Hui Ma,<sup>1</sup> Jinling Yu,<sup>1</sup> and Yu Liu<sup>1</sup>*Key Laboratory of Semiconductor Material Science, Institute of Semiconductors, Chinese Academy of Sciences, 100083 Beijing, China.*

(Dated: 4 December 2018)

In this work we investigated the InAs/InAlAs quantum wires (QWRs) superlattice by optically exciting the structure with near-infrared radiation. By varying the helicity of the radiation at room temperature we observed the circular photogalvanic effect related to the  $C_{2v}$  symmetry of the structure, which could be attributed to the formation of a quasi two-dimensional system underlying in the vicinity of the QWRs pattern. The ratio of Rashba and Dresselhaus terms shows an evolution of the spin-orbit interaction in quasi two-dimensional structure with the QWR layer deposition thickness.

---

<sup>a)</sup>yhchen@semi.ac.cn

In the last decade self-assembly grown nanostructures have attracted much research interest<sup>1-5</sup>. The self-assembled InAs quantum wires (QWRs) superlattice is one of the novel structures, which are smaller in size compared with some other nano wires and thus exhibit quantum phenomena. Precursors have done much work on these structures in the aspects of growing technique<sup>3-5</sup>, microscopy and optical spectroscopy. However, InAs is of great interest due to its high mobility, narrow band gap and large spin-orbit interaction. Much investigation with respect to these properties could be enrolled.

Considering the alignment of the QWRs which is responsible for the anisotropy of optical and electrical properties, we could invoke some techniques with respect to the symmetry. Photogalvanic effect<sup>6-11</sup> provides us such a way to investigate the symmetry of the structure and also the spin or orbital behavior of the charge carriers. The phenomena of photogalvanic effect is the generation of a direct electric current induced by homogenous radiation in a homogenous sample. Photogalvanic effect arises due to the absence of an inversion center in a crystal lattice. If the radiation is circularly polarized, it is called circular photogalvanic effect (CPGE). The CPGE current in a two-dimensional system of  $C_{2v}$  symmetry can be written as<sup>6,7</sup>

$$j_{C,y} = e\tau_p \frac{\gamma_{yx}}{\hbar} \frac{\alpha(\lambda)I}{\hbar\omega} P_c \hat{e}_x, \quad (1)$$

where  $\tau_p$  is a typical momentum relaxation time,  $\alpha(\lambda)$  is the absorption coefficient,  $I$  is the intensity of the radiation,  $P_c$  describes the helicity of the radiation and  $\hat{e}_x$  is the  $x$  component of the unit vector of the electric field amplitude.  $\gamma_{yx}$  is a second-rank pseudo-tensor which correlates the helix excitation  $P_c$  with the direct current  $j_{C,y}$ . Further details of CPGE in two-dimensional QWs can be find in Ref. 6 and 12. In a two-dimensional electron system, structure and bulk inversion asymmetry (SIA and BIA) contribute to the zero-field spin splitting. The SIA arises from the asymmetry in the grown direction of the structure, whereas the BIA arises from the absence of an inversion center. For a system of  $C_{2v}$  symmetry, the relative magnitude of SIA and BIA can be extracted via measuring the components of the current in different directions<sup>12</sup>, which demonstrates the property in terms of the spin-orbit interaction in the investigated low dimensional system.

Our QWRs samples are prepared by molecular-beam epitaxy (MBE) technique on semi-insulating (001)-oriented InP substrates. A 300nm InAlAs buffer layer and six periods of InAs-In<sub>0.52</sub>Al<sub>0.48</sub>As superlattice are deposited. In each period of the InAs-In<sub>0.52</sub>Al<sub>0.48</sub>As superlattice there is one QWR layer with a thickness of 2 ML, 4 ML or 6 ML respectively

for three samples and one unsymmetrical Si-doped InAlAs space layer. The Si donors are doped within layer with a thickness of 2 nm, which is sandwiched between a 4 nm and a 9 nm thick undoped InAlAs layer. The doping concentration is  $1 \times 10^{18} \text{ cm}^{-3}$ . An 80 nm thick InAlAs cap layer is grown on the most top. We cut the samples into  $10 \times 10 \text{ mm}^2$  in size and alloyed sixteen Ohmic contacts equidistantly on the edges (see Fig. 1). According to the TEM images of the same samples in Ref. 5, the QWRs are aligned along  $[1\bar{1}0]$ -direction. The photoluminescence and photocurrent spectroscopy results of the samples and detailed discussions can also be found in Ref. 5, which show that the sample with thicker QWR layers has a narrower size distribution of the wires and less defects.

The experimental setup is illustrated in Fig. 1. The near-infrared laser radiation for the optical excitation has a wavelength of  $1.06 \text{ }\mu\text{m}$  and a power of  $\sim 1 \text{ Watt}$ . A photoelastic modulator (PEM) is employed to convert the incoming linearly polarized light into a modulated circularly polarized light with a fixed modulating frequency at  $50 \text{ kHz}$ .

According to the working principle of the PEM, the electrical signals from the samples referenced to the base frequency correspond to the circular polarization, while those referenced to the second harmonic frequency correspond to the linear polarization. The electrical signals are therefore measured using standard lock-in technique. The total electric current is given by

$$j = j_{C(1f)} + j_{L(2f)} + j_0, \quad (2)$$

where  $j_{C(1f)}$  is the circular polarization contributed current,  $j_{L(2f)}$  is the linear polarization contributed current and  $j_0$  is the polarization independent current which can be extracted by invoking an optical chopper.

We firstly investigate the photoconductivities<sup>1,13,14</sup> of the samples in different directions in order to take the anisotropic absorbance into account. The photoconductivity reads

$$\Delta\sigma = \Delta n e \mu_n = [\alpha(\lambda) g I \tau_n] e \mu_n, \quad (3)$$

where  $\Delta n$  is the photogenerated excess carrier density,  $\alpha(\lambda)$  is the absorption coefficient,  $g$  is the generation rate of the carrier pairs,  $I$  is the intensity of light,  $\tau_n$  is the life time of the excess electrons,  $e$  is elementary charge and  $\mu_n$  is the mobility of the electrons. Since the mobility of holes is one order of magnitude lower than the electrons, the contribution of holes to the photoconductivity is omitted in Eq. 3. The investigation of photoconductivity is done by applying a DC-bias between the contacts and recording the current referenced to

the optical chopper on the load resistor. Since the photogalvanic effect is proportional to the absorbance and intensity of the radiation and the charge carrier density (See Eq. 1), we could normalized the photogalvanic voltage by the photoconductivity so that the photogalvanic currents in different directions are comparable without referring to the anisotropic optical excitation.

The investigation of photogalvanic effect is carried out at room temperature by varying the azimuth angle  $\beta$  of the incident light, where the azimuth angle  $\beta$  (See Fig. 1) is the angle between the plane of incidence and the alignment of the QWRs. We vary  $\beta$  by rotating the sample and measure the photocurrents both perpendicular and parallel to the plane of incidence. The CPGE currents are shown in Fig. 3. The experimental results of the azimuth angle dependence of the CPGE current can be well fitted by

$$j_{C,y} = a_0 + a_1 \cos 2\beta, \quad (4)$$

where  $a_0$  and  $a_1$  are fitting parameters. In  $[1\bar{1}0]$  direction, which is parallel to the alignment of the QWRs, the current  $j_{C,y}$  reaches minima. In  $[110]$  direction, the  $j_{C,y}$  is maximum. The results well demonstrate that the electrons are not confined in a single wire but move in two dimensions. We could extract the symmetric and anti-symmetric contributions of the CPGE as a function of the azimuth angle. Compared with the two-dimensional structure of  $C_{2v}$  symmetry in the same framework as described in Ref.<sup>12</sup>, we find that the current behaves similar to that in the two-dimensional system. Thus, we suggest that the CPGE current is induced in a quasi two-dimensional structure of  $C_{2v}$  symmetry in the vicinity of the QWRs and subjected to an influence of the QWRs pattern in terms of the anisotropic absorption. Therefore, we can also study the structure and bulk inversion asymmetry (SIA and BIA)<sup>12,15</sup> in this quasi two-dimensional structure.

By taking the ratio of  $a_0$  and  $a_1$ , we can obtain the ratio of Rashba and Dresselhaus terms<sup>9,16</sup> of the quasi two-dimensional system

$$\frac{R}{D} = \frac{a_0}{a_1}, \quad (5)$$

where  $R$  is the Rashba coefficient and  $D$  is the Dresselhaus coefficient. The ratios  $R/D$  in different samples are summarized in Table I. Since the samples differ from one another only in the deposition thickness of QWRs, the ratios of the SIA and BIA terms imply an interplay of the QWRs structure and the quasi two-dimensional system. As the thickness of

the QWR layer increasing, the  $R/D$  ratios decrease, which indicates either a decrease of the SIA or an increase of BIA. Since the samples only differ with one another in the size of the QWRs, whereas the  $\delta$ -doping positions are the same, the difference of the  $R/D$  ratios comes from the coupling between the QWRs pattern and the quasi two-dimensional structure. The patterning effect imposed by the QWRs modulates the zero-field spin splitting in terms of the ratio of Rashba and Dresselhaus terms.

The band gap of InAs bulk material is 0.354 eV, which is smaller than the photon energy of the 1.064  $\mu\text{m}$  radiation (1.19eV). The microscopic mechanism of optical transition induced by the 1.064  $\mu\text{m}$  radiation can be addressed to the interband regime, where the electrons in the valence band absorb the photon energy and transit to a higher level in the conductance band. According to Ref. 5, the photoluminescence spectra show that the PL peak of the structure with thicker InAs QWR layer has a lower energy and smaller energy broadening, which indicates that the size fluctuation decreases with increasing InAs deposition thickness. Accordingly, the electron could be more localized as the increasing InAs deposition thickness. However, since the excitation energy is sufficiently high, photogenerated carriers could be induced in some kind of quasi two-dimensional structure in the vicinity of the QWRs, for instance, the wetting layer between the buried InAs wires and the  $\text{In}_{0.52}\text{Al}_{0.48}\text{As}$  barrier. The electron wave function in a single InAs wire couples with its neighbors. Thus, the resistances do not differ identically in different directions (See Fig. 2(a)). The electrons are free to move in two dimensions but subjected to the anisotropic influence of the QWRs pattern in terms of the absorbance.

In summary, we observed the circular photogalvanic effect in the InAs QWRs patterned quasi two-dimensional structure under 1.064  $\mu\text{m}$  near-infrared radiation. The current exhibits anisotropy with respect to the alignment of the QWR pattern. The investigation of the ratio of Rashba and Dresselhaus terms demonstrates a modulation of the spin-orbit interaction in the quasi two-dimensional system by the QWRs pattern as the increasing deposition thickness.

## ACKNOWLEDGMENTS

This work is supported by the National Natural Science Foundation of China (60625402, 60990313). C.Y. Jiang also thanks J. Karch and S.D. Ganichev in Regensburg Terahertz

Center for fruitful discussions.

## REFERENCES

- <sup>1</sup>A. Patanè, A. Levin, A. Polimeni, L. Eaves, P. C. Main, M. Henini, and G. Hill, “Carrier thermalization within a disordered ensemble of self-assembled quantum dots,” *Phys. Rev. B* **62**, 11084–11088 (2000).
- <sup>2</sup>F. Fossard, A. Helman, G. Fishman, F. H. Julien, J. Brault, M. Gendry, E. Péronne, A. Alexandrou, S. E. Schacham, G. Bahir, and E. Finkman, “Spectroscopy of the electronic states in inas quantum dots grown on  $\text{In}_x\text{Al}_{1-x}\text{As}/\text{InP}(001)$ ,” *Phys. Rev. B* **69**, 155333 (2004).
- <sup>3</sup>Y.-L. Wang, Y.-H. Chen, J. Wu, W. Lei, Z.-G. Wang, and Y.-P. Zeng, “Structural and optical properties of  $\text{InAs}/\text{In}_{0.52}\text{Al}_{0.48}\text{As}$  self-assembled quantum wires on  $\text{InP}(001)$ ,” *Journal of Crystal Growth* **284**, 306–312 (2005).
- <sup>4</sup>W. Lei, Y. H. Chen, P. Jin, X. L. Ye, Y. L. Wang, B. Xu, and Z. G. Wang, “Shape and spatial correlation control of  $\text{InAs-InAlAs-InP}(001)$  nanostructure superlattices,” *Applied Physics Letters* **88**, 063114 (2006).
- <sup>5</sup>W. Lei, Y. H. Chen, Y. L. Wang, X. Q. Huang, C. Zhao, J. Q. Liu, B. Xu, P. Jin, Y. P. Zeng, and Z. G. Wang, “Optical properties of self-assembled  $\text{InAs}/\text{InAlAs}/\text{InP}$  quantum wires with different inas deposited thickness,” *Journal of Crystal Growth* **286**, 23–27 (2006).
- <sup>6</sup>S. Ganichev and W. Prettl, “Spin photocurrents in quantum wells,” *Journal of Physics-Condensed Matter* **15**, R935–R983 (2003).
- <sup>7</sup>E. L. Ivchenko, “Circular photo-galvanic and spin-galvanic effects,” (Springer, 2005) Chap. 658, pp. 23–50.
- <sup>8</sup>E. L. Ivchenko and S. D. Ganichev, “Spin physics in semiconductors: Spin-photogalvanics,” (Springer, 2008) Chap. 9, pp. 245–277.
- <sup>9</sup>E. Ivchenko, *Optical Spectroscopy of Semiconductor Nanostructures* (Alpha Science Int., Harrow, UK, 2005).
- <sup>10</sup>V. Lechner, L. E. Golub, P. Olbrich, S. Stachel, D. Schuh, W. Wegscheider, V. V. Bel’kov, and S. Ganichev, “Tuning of structure inversion asymmetry by the delta-doping position in (001)-grown gaas quantum wells,” *Appl. Phys. Lett.* **94**, 242109 (2009).
- <sup>11</sup>P. Olbrich, E. L. Ivchenko, R. Ravash, T. Feil, S. D. Danilov, J. Allerdings,

- D. Weiss, D. Schuh, W. Wegscheider, and S. D. Ganichev, “Ratchet effects induced by terahertz radiation in heterostructures with a lateral periodic potential,” *Phys. Rev. Lett.* **103**, 090603 (2009).
- <sup>12</sup>S. Giglberger, L. E. Golub, V. V. Bel’kov, S. N. Danilov, D. Schuh, C. Gerl, F. Rohlfiing, J. Stahl, W. Wegscheider, D. Weiss, W. Prettl, and S. D. Ganichev, “Rashba and dresselhaus spin splittings in semiconductor quantum wells measured by spin photocurrents,” *Phys. Rev. B* **75**, 035327 (2007).
- <sup>13</sup>K. W. Berryman, S. A. Lyon, and M. Segev, “Mid-infrared photoconductivity in inas quantum dots,” *Appl. Phys. Lett.* **70**, 1861 (1997).
- <sup>14</sup>L. Chu, A. Zrenner, G. Böhm, and G. Abstreiter, “Lateral intersubband photocurrent spectroscopy on InAs/GaAs quantum dots,” *Appl. Phys. Lett.* **76**, 1944 (2000).
- <sup>15</sup>Y. V. Pershin and C. Piermarocchi, “Spin photovoltaic effect in quantum wires with rashba interaction,” *Appl. Phys. Lett.* **86**, 212107 (2005).
- <sup>16</sup>S. D. Ganichev, V. V. Bel’kov, L. E. Golub, E. L. Ivchenko, P. Schneider, S. Giglberger, J. Eroms, J. D. Boeck, G. Borghs, W. Wegscheider, D. Weiss, and W. Prettl, “Experimental separation of rashba and dresselhaus spin splittings in semiconductor quantum wells,” *Phys. Rev. Lett.* **92**, 256601 (2004).

TABLE I. Ratio of Rashba and Dresselhaus terms

Thickness of a QWR layer (ML)	2	4	6
Average width of a QWR (nm)	11.8	14.4	16.7
Average height of a QWR (nm)	3.8	4.7	5.6
Ratio of SIA and BIA ( $R/D$ )	1.50	1.29	1.25

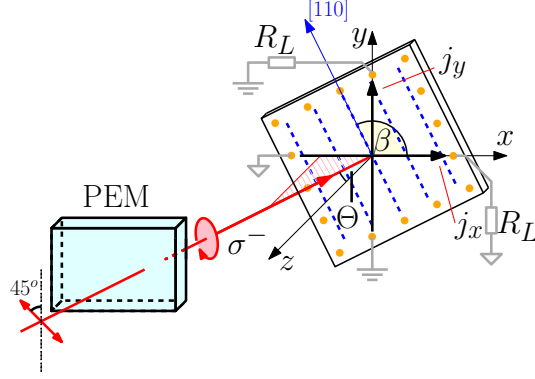


FIG. 1. Experimental setup. The sample plane lies in the  $x - y$  plane and the  $x - z$  plane is always the plane of incidence.  $j_x$  and  $j_y$  are the  $x$  and  $y$  components of the current respectively.  $\Theta$  is the angle of incidence between the incident light and the  $z$  axes.  $\beta$  is the azimuth angle, which is between the orientation of QWRs and  $x$  axes. Any component of the current  $j_\alpha$  (The index  $\alpha$  refers either  $x$  or  $y$  with respect to the coordinate system) is calculated using the formula  $j_\alpha = \frac{\Delta V_\alpha}{R_L}$ , where  $\Delta V_\alpha$  is the electric potential difference between the two measured contacts,  $R_L$  is the load resistance with a value of 15 k $\Omega$ .

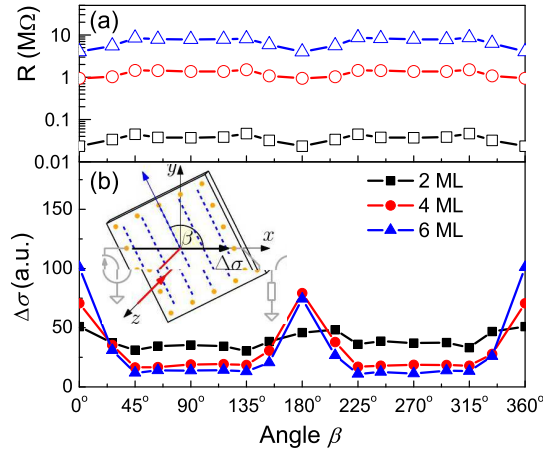


FIG. 2. Resistance (a) and photoconductivity (b) of the samples as a function of the azimuth angle  $\beta$ . The squares, circles and triangles stand for the experimental data of the sample with 2 ML, 4 ML and 6 ML thickness of QWR layer, respectively.

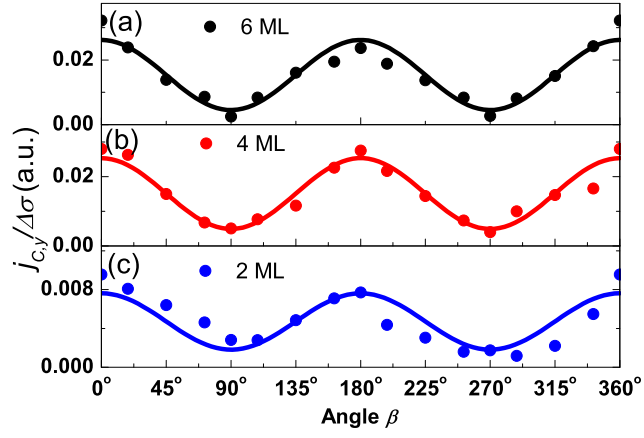


FIG. 3. CPGE current  $j_y$  (See Fig. 1 for the definition of the coordinate) with QWR layer thickness: (a) 2 ML, (b) 4 ML, (c) 6 ML as a function of azimuth angle  $\beta$ . The solid lines are the fitting curves. The angle of incidence is  $30^\circ$ .